High-field magnetoresistance in nanowire organic spin valves

K. M. Alam and S. Pramanik*

Department of Electrical and Computer Engineering, University of Alberta, Edmonton, Canada AB T6G 2V4

(Received 15 January 2011; revised manuscript received 25 April 2011; published 23 June 2011)

In this paper, we report high-field magnetoresistance measurements on template-grown *nanowire* organic spin valves in which tris-8 hydroxyquinoline aluminum (Alq_3) is sandwiched between two ferromagnetic electrodes: nickel (Ni) and cobalt (Co). We report a magnetoresistance effect in which the resistance changes considerably in the field range where both ferromagnets have parallel magnetizations. We show that this effect does not originate from organic magnetoresistance or the anisotropic magnetoresistance effect of the ferromagnets. Instead, the observed effect can be explained by invoking magnetic-field-dependent spin-diffusion length, where spin diffusion takes place primarily via the Elliott-Yafet mode. These data support the view expressed by some previous reports that Elliott-Yafet is the dominant spin-relaxation mode in template-grown organic nanowires.

DOI: 10.1103/PhysRevB.83.245206 PACS number(s): 72.25.Rb, 72.25.Mk, 72.25.Hg, 72.25.Dc

I. INTRODUCTION

In recent years, spin transport in organic π-conjugated semiconductors has become a topic of significant interest since these materials typically offer long spin lifetime, which is desirable for many spintronic applications such as organic nonvolatile memory, single spin logic, and spin-based organic light-emitting diodes.[1–4] Several studies have been reported with the aim to understand spin injection and transport in this new class of materials. The optical pump-probe method, which has been applied successfully for studying spin transport in inorganic semiconductors, is not suitable for organics due to their weak spin-orbit interaction.[5,6] Recently, several other techniques have been developed for studying spin injection and transport in organics. These include (a) muon spin rotation (μSR) spectroscopy,[7,8] (b) spin-polarized photoemission spectroscopy,[9] and (c) spin-polarized scanning tunneling microscopy.[10,11] However, due to the complexity and lack of wide availability of these techniques, the majority of the spin-transport experiments in organics still employ a spin-valve geometry in which the organic layer is sandwiched between two ferromagnetic electrodes.[12–25] Using a so-called modified Jullière formula,[13,15] it is possible to estimate the *lower bound* of spin-diffusion length from the spin-valve signals. By using this information in conjunction with the mobility data, one can also estimate the lower limit of the spin-diffusion time.[15] Combining spin-valve response with the spectroscopic information provides an overall picture of spin injection and transport in organic-based systems.[8]

Arguably, Alq_3 (tris-8 hydroxyquinoline aluminum), which is widely used in organic light-emitting diodes as the electron-transporting and light-emitting layer, is the most studied material so far in the context of spin injection and transport in organics. Various spin-valve geometries have been investigated, which include (a) Alq_3 thin films (e.g., Refs. 13, 17, and 18), (b) tunnel barriers (e.g., Refs. 14, 21, and 22), and (c) nanowires.[15,16] Different types of magnetic materials, such as transition metals,[14–16,18] half-metallic ferromagnets,[12,13,22] and organic magnetic semiconductors[26] have been employed as spin injector and detector.

In spite of this huge body of work, there still exists significant controversy regarding the dominant spin-relaxation mechanism of charge carriers in organics, especially Alq_3. Two possible agents[27] are the Elliott-Yafet mechanism (which originates from the spin-orbit interaction)[28] and hyperfine interaction with nuclei.[29,30] We note that the mechanisms such as Elliott-Yafet, D'yakonov-Perel',[31] Bir-Aronov-Pikus,[32] and hyperfine interaction were originally developed to understand the spin-relaxation mechanisms in periodic inorganic solids. While the expressions for the spin-relaxation rate derived in these works can not be directly applied for disordered organic solids, the physical pictures offered by these models still remain valid. For example, charge transport in organics often takes place via hopping and D'yakonov-Perel' spin relaxation has indeed been modeled for hopping transport.[33] Therefore, we will continue to use the above-mentioned mechanisms to discuss spin relaxation in organic solids.

The origin of the Elliott-Yafet mechanism (for both ordered and disordered semiconductors) lies in the fact that, in the presence of spin-orbit interaction, electronic states are not spin eigenstates. Spin-orbit interaction "mixes" the spin-up and spin-down states where spin-up (down) is defined with respect to some suitable quantization axis. The recently proposed "charge-induced spin-polarization" mechanism[34] or an external magnetic field can also contribute to spin mixing in an organic semiconductor. Therefore, even spin-independent momentum scattering events (or hopping for disordered organics) are naturally accompanied by spin scattering. The corresponding spin-relaxation rate (for organic solids) has recently been calculated in Ref. 35.

In the case of hyperfine interaction, at each molecular site, carrier spins precess about the effective magnetic field due to the hyperfine fields of the hydrogen nuclei and the external magnetic field. The hyperfine field is random in nature, so as the carrier hops through various molecular sites, its spin precesses about different axes, which causes relaxation of the injected spin polarization.[36]

The effect of hyperfine interaction on organic magnetoresistance (OMAR) property of Alq_3 has been studied in Ref. 37. In this paper, OMAR response was measured with protonated and deuterated Alq_3, which have very different strengths of hyperfine coupling. However, no significant difference in OMAR response was observed, indicating that hyperfine interaction may not play a dominant role in determining spin-dependent properties in Alq_3. However, hyperfine interaction

may play a major role in some other organic polymer such as DOO-PPV.[23]

Spin-orbit interaction is commonly assumed to be very weak in Alq_3 since its major constituents are light elements with low atomic number and the strength of spin-orbit coupling is proportional to the fourth power of the atomic number. We note that such an argument generally fails for other low atomic number systems such as carbon nanotubes[38] and that the strength of the Elliott-Yafet mechanism also depends on carrier scattering (or hopping) rate and is enhanced in poor mobility systems.[39] Thus, even if we assume that spin-orbit interaction is weak in organics, the Elliott-Yafet mechanism can still play a dominant role in *low-mobility* organics. This is most likely the case for Alq_3 nanowires embedded in an alumina template.[15,16] In this system, the carrier mobility is much lower due to additional scattering in the presence of charged surface states and the Elliott-Yafet mechanism can play a dominant role. Dependence of spin-relaxation length on temperature, bias, and mobility agrees with this observation.[15,40]

In Ref. 16, we carried out an exhaustive study of nanowire organic spin-valve structures and reported occurrence of both normal and inverse spin-valve effects in these devices. Sign inversion of the spin-valve signal occurs due to resonant tunneling through localized impurity states in the organic semiconductor that effectively flips the polarization of one of the ferromagnets. This has also been confirmed later by other groups.[10,11,22] Surprisingly, in the nanowire samples, the sign of the spin-valve signal was found to be correlated with the background magnetoresistance of the device: the normal spin-valve effect is always found to be accompanied by a positive background magnetoresistance and the inverse effect is accompanied by a negative background magnetoresistance.[16] This correlation can be explained within the framework of spin injection and transport in Alq_3, where the transport is dominated by the Elliott-Yafet mode.[16]

To further examine the validity of this model, in this paper, we investigate *high-field*-magnetoresistance measurements on nanowire organic spin valves [nickel (Ni)/tris-8 hydroxyquinoline aluminum (Alq_3)/cobalt (Co)] since the Elliott-Yafet mode and the hyperfine interaction have opposite dependence on magnetic field. For the Elliott-Yafet mode, spin-relaxation (or -diffusion) length decreases with increasing magnetic field due to enhanced spin mixing in the presence of spin-orbit interaction.[16] The opposite dependence is observed for hyperfine interaction in which case high magnetic field effectively pins the carrier spin polarizations, thereby enhancing the spin-relaxation length.[36]

In this paper, we report a magnetoresistance effect in the high-magnetic-field regime where the ferromagnetic spin injectors and detectors have parallel magnetization. We show that this behavior can not be explained by effects such as organic magnetoresistance or anisotropic magnetoresistance of the ferromagnets. We find that, for nanowires, contrary to some thin-film geometries,[13,41] magnetoresistance tends to saturate at high field in the low-temperature regime where spin injection is significant. We show that these data can be explained qualitatively by invoking a magnetic-field-dependent spin-relaxation length, where spin relaxation primarily takes place via the Elliott-Yafet mode.[15,16,40]

This paper is organized as follows. We first briefly describe the physics of the organic spin-valve device and the possible origins of the background magnetoresistance and sign inversion of the spin-valve peaks. In Sec. III, we describe the fabrication of the nanowire spin valves and the control samples. The results and discussion are presented in Sec. IV, and we conclude in Sec. V.

II. ORGANIC SPIN VALVES AND BACKGROUND MAGNETORESISTANCE

A. Normal and inverse spin-valve effects

An *organic* spin valve is a trilayered construct in which an organic "active" layer is contacted by two ferromagnetic electrodes of different coercivities. Both small molecular weight organics and long chain polymers have been reported in literature in lateral and vertical geometries. Since Alq_3 belongs in the category of small molecular weight organics, in the following discussion we assume the transport model for this class of organics.

Unlike giant magnetoresistive devices, the ferromagnetic contacts in a spin-valve device are not magnetically coupled with each other. As a result, their magnetizations can be independently controlled by a global magnetic field. One of these ferromagnets acts as spin injector, i.e., under an applied electrical bias, it injects spin-polarized carriers (from the quasi-Fermi level, which in the case of ferromagnets have unequal density of states for spin-up and spin-down electrons) into the organic layer. Efficient spin injection has been reported for the cases when there exists an interfacial tunnel barrier[17] or even a magnetically dead layer[18] between the injector ferromagnet and the organic layer. Next, the injected spin-polarized carriers travel through the organic layer under the influence of the transport driving electric field. For small molecular weight organics, carrier transport mainly occurs via hopping through molecular and defect states.[25,36,40] During this transit, different spins interact with their environments differently via spin-orbit or hyperfine interactions and their original spin orientations change by various amounts. This leads to a gradual loss of the injected spin polarization, which is termed as spin relaxation. The second ferromagnet also provides unequal spin-up and spin-down density of states at the quasi-Fermi level and preferentially transmits spins of one particular orientation.

For simplicity of discussion, let us assume that the injector (detector) ferromagnet preferentially injects (transmits) majority spins, which is the case for Ni and Co electrodes.[42] The transmission probability (T) of a carrier through the detector is proportional to $\cos^2(\theta/2)$, where θ is the angle between the spin orientation of the carrier arriving at the detector interface and the magnetization of the detector ferromagnet.[43] This means that, if the magnetizations of the ferromagnets are parallel and spin-diffusion length is much larger than the thickness of the organic layer (i.e., the carriers partially retain their initial spin orientation), the transmission probabilities of the carriers arriving at the detector interface should be close to unity (since $\theta \approx 0$), which will result in a small device resistance (say R_P). Similarly, when the magnetizations are antiparallel, the transmission probabilities should be close to zero (since $\theta \approx \pi$), and in this case, one should observe

large device resistance (say R_{AP}). In this situation, $R_{AP} > R_P$ and this is known as the "normal" spin-valve effect. In the magnetoresistance plot, the resistance peak occurs between the coercive fields of the ferromagnets where their magnetizations are antiparallel.

It follows that, if only one of the ferromagnets preferentially transmits (either injects or detects) minority spins, then resistance of the spin valve will be large (small) in parallel (antiparallel) configurations. This is sometimes referred to as the inverse spin-valve effect. Interestingly, in the case of (pinhole-free) organic layer, sign inversion of the spin-valve peaks also occurs when *both* ferromagnets transmit either spin-up or spin-down electrons. This has been observed in case of Ni-Alq_3-Co nanojunction devices where both nickel and cobalt are the majority spin injector.[16] Moreover, in such cases, both normal and inverse spin-valve effects are observed for nominally identical samples under the same temperature and bias.[15,16] In such cases, the inverse effect occurs if the carrier tunnels resonantly through an impurity state, which inverts the effective spin polarization of the ferromagnet nearest to the impurity. This has been discussed in Refs. 16 and 22.

B. Background magnetoresistance

In many cases (and especially for nanowires), the spin-valve signal is superimposed on a background magnetoresistance. Depending on the system under consideration, this can originate from various sources such as (a) the intrinsic magnetoresistance of organic semiconductors (organic magnetoresistance or OMAR),[44,45] (b) magnetic-field-dependent spin injection in organics,[41] and/or (c) magnetic-field dependence of the spin-diffusion length.[36]

If the OMAR effect is dominant, then nominally identical spin-valve specimens should exhibit qualitatively similar background magnetoresistance for a fixed temperature and bias since OMAR is not directly dependent on spin injection and detection. No sign inversion of the background signal is expected between normal and inverse spin-valve devices under identical operating conditions. This feature can be used to investigate if the observed background magnetoresistance has any connection with OMAR. In our nanowire devices, we observed both positive and negative background magnetoresistance for nominally identical samples under the same operating conditions (discussed later). This indicates that OMAR is not the origin of the observed background magnetoresistance.

Magnetic-field-dependent spin injection is the major cause for background magnetoresistance in devices where half-metallic ferromagnets are employed as spin injector and detector.[41] Such an effect is unlikely for transition metal ferromagnets as is the case here and in our earlier work.[15,16] Therefore, our data can only be explained by invoking a magnetic-field-dependent spin-diffusion length. Our data indicate that the spin diffusion (or relaxation) occurs primarily via the Elliott-Yafet mode, for which spin-diffusion length decreases with increasing magnetic field.

It is to be noted that the background magnetoresistance and spin-valve-type signal can also originate due to a local Hall effect caused by the fringing magnetic fields of the ferromagnets or magneto-Coulomb effect. In such cases, the magnetoresistance and spin-valve peaks are unrelated to spin injection and transport and should persist even when a *single* contact is ferromagnetic. These control experiments need to be performed to verify if the observed features in magnetoresistance are indeed due to spin-related effects. For the reported nanowire samples, as we will show below, the magnetoresistance features are absent when a single contact is ferromagnetic. Therefore, the observed magnetoresistance behavior must originate from the magnetic-field dependence of spin-diffusion length.

III. EXPERIMENT

We use a nanoporous alumina (aluminum oxide) template for fabrication of the *nanowire* organic spin valves. This method has been adopted before by many groups to fabricate various nanostructures with widely tunable aspect ratio.[46] The template-grown nanowires, if not released from the host alumina matrix, typically show low mobility due to scattering from a large number of charged surface states. This method therefore allows reducing the mobility without sacrificing the material quality. The resistance of a single spin-valve nanowire is generally very high (~ 100 GΩ), but multiple ($\sim 10^8$) nanowires can be connected in parallel to significantly reduce the overall device resistance. Note that, in this approach, the nanowires are grown in parallel under identical environment and the individual nanowires are nominally identical.

The anodic alumina template, which contains a hexagonally ordered array of cylindrical nanopores with diameter ~ 50 nm, length 1μm, and pore density $\sim 2 \times 10^{10}/\text{cm}^2$ is synthesized by an electrochemical self-assembly technique on a high-purity (99.997%) aluminum substrate. The pore bottoms are generally blocked by a continuous nonporous barrier layer of aluminum oxide. This insulating alumina layer can be etched away preferentially (without destroying the porous structure) to expose the pore bottoms to the underlying aluminum substrate. Such treatment is beneficial for the transport experiment since aluminum substrate can now act as a back contact for the materials deposited inside the pores. Figure 1(a) shows the field-emission scanning electron microscopic (FESEM) image of the template in which cylindrical nanopores are clearly visible.

For the fabrication of nanowire Alq_3 spin valves, we first electrodeposit nickel at the bottom of the pores from a slightly acidic aqueous bath of nickel sulfate. This nickel layer generally forms an ohmic contact with the underlying aluminum substrate and exhibits linear current-voltage characteristics (not shown). A thin layer (~ 30 nm) of Alq_3 is vacuum evaporated (10^{-6} Torr) on top of nickel through a shadow mask of area ~ 1 mm^2, followed by deposition of cobalt, without breaking the vacuum. Thus, we obtain an array of nominally identical spin-valve nanowires. The areal density of the vertically standing nanowires is 2×10^{10} /cm^2. Since the cobalt contact pad has an area of ~ 1 mm^2, approximately 2×10^8 nanowires are electrically contacted. Figure 1(b) shows the schematic depiction of the device. Further details of the fabrication process have been reported before in Ref. 16.

The equivalent resistor model of the device is shown in Fig. 1(c). From this model, since R_{Ni}, R_{Co}, $R_{\text{Al}} \ll R_{\text{Alq}_3} \ll R_{\text{Al}_2\text{O}_3}$, we effectively measure the resistance of the Alq_3 layer

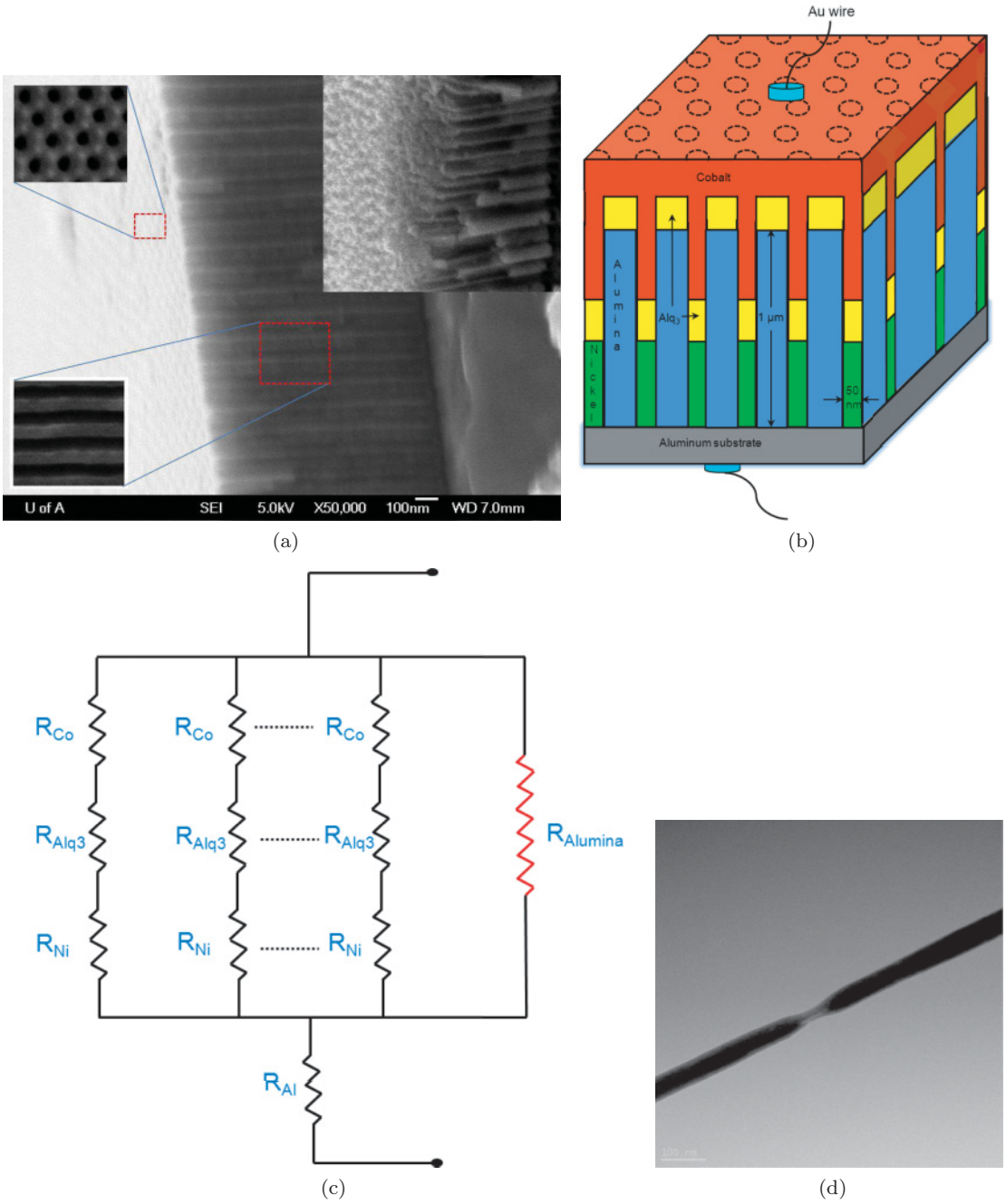

FIG. 1. (Color online) (a) Field-emission scanning electron microscopic (FESEM) image of the nanoporous alumina template. The array of cylindrical pores is clearly visible. The pore density is $\sim 10^{10}/\text{cm}^2$. The top-right inset shows the electrodeposited ferromagnetic nanowire contacts. (b) A schematic description of the spin-valve device, which consists of an array of nominally identical nanowire spin valves. (c) A resistor model of the device in (b), with R_x representing the resistance of the layer x ($x \equiv$ Ni, Co, Al, Alq_3, alumina). Since R_{Ni}, R_{Co}, $R_{Al} \ll R_{Alq_3} \ll R_{alumina}$, we effectively measure the resistance of the Alq_3 layer between the top and bottom terminals. (d) Transmission electron micrograph of a single nanowire spin valve. The light colored region at the center is the Alq_3 layer.

sandwiched between the top (Co) and bottom (Ni) terminals. The overall device resistance is ~ 1 kΩ at low temperature and low bias (see later), which implies that the resistance of a single spin-valve nanowire is ~ 200 GΩ, which is beyond the instrument limits.

As discussed in earlier works,[15,16,40] in contrast to direct evaporation, the template-based fabrication process produces a pinhole and metal filament-free organic layer. This is presumably because the alumina pillars surrounding the embedded Alq_3 layers prohibit direct impingement of the cobalt atoms on the Alq_3 layers and also shadow the Alq_3 layers from the radiation of the evaporation source. This spatial separation of the "accommodation phase" of the Co deposition process from the organic layer remotely dissipates the kinetic energy

and the heat of condensation.[47] The interfacial cobalt layer is formed by Co atoms arriving at the Alq_3 surface via surface diffusion on the alumina surface.[15] This significantly reduces the degree of cobalt interdiffusion into the organics since the activation energy for surface diffusion is typically much lower than the binding energy.[47] The pinhole-free feature is directly visible from the nonlinear current-voltage characteristics.[15] The transmission electron microscopy (TEM) image of a single spin-valve nanowire is shown in Fig. 1(d).

The magnetoresistance is measured with an ac bias current of 10 μA rms over a magnetic-field range of 0–70 kOe in a temperature range of 1.9–10 K. Note that such high-field data on organic nanowire spin-valve samples have not been reported so far, although they can potentially shed some light on the underlying spin-relaxation mechanism in organics.

To ensure that the high-field-magnetoresistance behavior originates from the organics and not from the ferromagnetic contacts, we prepared a separate set of control samples (C_1) without the organic layer. High-field magnetoresistance of these bilayered Ni/Co samples was measured under the same conditions of the spin-valve samples. In another set of control samples (C_2), the top Co layer was replaced by silver, resulting in Ag/Alq_3/Ni structures. These devices do not show any spin-valve effect or background magnetoresistance. As we will show in the next section, comparison of these data confirms that the observed magnetoresistance effect is indeed due to spin injection and transport in the Alq_3 layer.

IV. RESULTS AND DISCUSSION

A. Low-temperature measurement

In this paper, we perform the magnetoresistance measurements at a low-temperature range of $\lesssim$10 K due to the following reasons:

(a) Hyperfine interaction is stronger in the low-temperature regime due to two reasons. First, as the temperature is increased, the nuclear spin system gradually loses the net spin polarization with a concomitant weakening of the effective hyperfine magnetic field.[29,30] Second, and more importantly, the hopping frequency (ω_{ij}) of the charge carriers between the neighboring molecular sites (i and j) is given by $\omega_{ij} \propto \exp[-(\epsilon_j - \epsilon_i)/k_B T]$, where $\epsilon_{i(j)}$ represents the on-site energies of site $i(j)$ with $\epsilon_j > \epsilon_i$, k_B is the Boltzmann's constant, and T is the temperature.[36] Increasing temperature therefore leads to higher hopping frequency and lower waiting time at the molecular sites, which further reduces the effectiveness of hyperfine interaction in spin relaxation.[36] On the other hand, frequent hopping strengthens the Elliott-Yafet mode, since each hopping event is associated with reorientation of carrier spins. Therefore, the presence of hyperfine interaction should be relatively easily detectable in the low-temperature regime. If hyperfine interaction is dominant in this temperature range, magnetoresistance measurements should show corresponding magnetic-field dependence. If such behavior is not observed, we can safely rule out hyperfine interaction as the dominant source of spin relaxation at *any* temperature.

(b) It is well known that the *surface* spin polarization (and not bulk spin polarization) of a transition metal ferromagnet is mainly responsible for spin injection and has a much stronger temperature dependence than bulk spin polarization.[18,48] Surface spin polarization is also strongly dependent on the material grown on the ferromagnet.[48] This is mainly the reason why organic spin valves that use transition metal ferromagnets (and no additional interfacial spin-injection enhancing layer, see e.g., Refs. 17 and 18) are only operative at $\lesssim$100 K, even though the Curie temperature of the ferromagnets is much larger.[15,16,18,48,49] Limiting the operating temperature within a relatively low range of $\lesssim$10 K enables us to obtain significant spin injection in our samples, which manifests in a strong spin-valve peak. This also minimizes the possibility of magnetoresistance artifacts, which can arise at higher temperatures due to degraded interface quality. The observed low-temperature magnetoresistance behavior, with suitable control experiments, can therefore be explained in terms of spin injection and transport.

B. Low-field magnetoresistance

Figure 2 shows the typical low-field-magnetoresistance measurements on Ni-Alq_3-Co *nanowire* spin valves. These data are similar to those reported earlier[15,16] and show the typical spin-valve peaks [Fig. 2(a), normal spin-valve effect with $R_{AP} > R_P$] or troughs [Fig. 2(b), inverse spin-valve effect with $R_{AP} < R_P$] within the coercive fields of nickel and cobalt nanowire contacts (800 and 1800 Oe, respectively). These peaks, combined with suitable control experiments (described below), indicate spin injection and transport in the organic layer.

One crucial feature in Fig. 2 is the correlation between the sign of the spin-valve signal and the sign of the background magnetoresistance. For the devices showing normal spin-valve effect, the background magnetoresistance is positive [i.e., resistance increases with the magnitude of the magnetic field, as shown in Fig. 2(a)] and for the devices showing inverse spin-valve effect, the background magnetoresistance is negative [i.e., resistance decreasing with the magnitude of the magnetic field, as shown in Fig. 2(b)]. As discussed before, this sign difference between nominally identical samples, tested under nominally identical temperature and bias conditions, can not be explained by organic magnetoresistance effect. This also rules out anisotropic magnetoresistance as a potential contributor. Later in this paper, we describe additional control experiments that will reconfirm these conclusions.

Another interesting difference between these two classes of samples, which is not understood at this point, is the value of the saturation magnetic field. For the normal spin-valve samples, the magnetoresistance does not saturate in the range of [−2,2] kOe, as shown in Fig. 2(a). Note that this range includes the coercive fields of the Ni and Co nanowire contacts, which are +(−)800 Oe and +(−)1800 Oe, respectively, so that the spin-valve signal is visible in the [−2,2] kOe range. The inverse spin-valve samples, on the other hand, show magnetoresistance saturation at a relatively low field of 2 kOe, soon after the magnetization of Co flips. In the following discussion, we therefore focus on the *high-field behavior* of

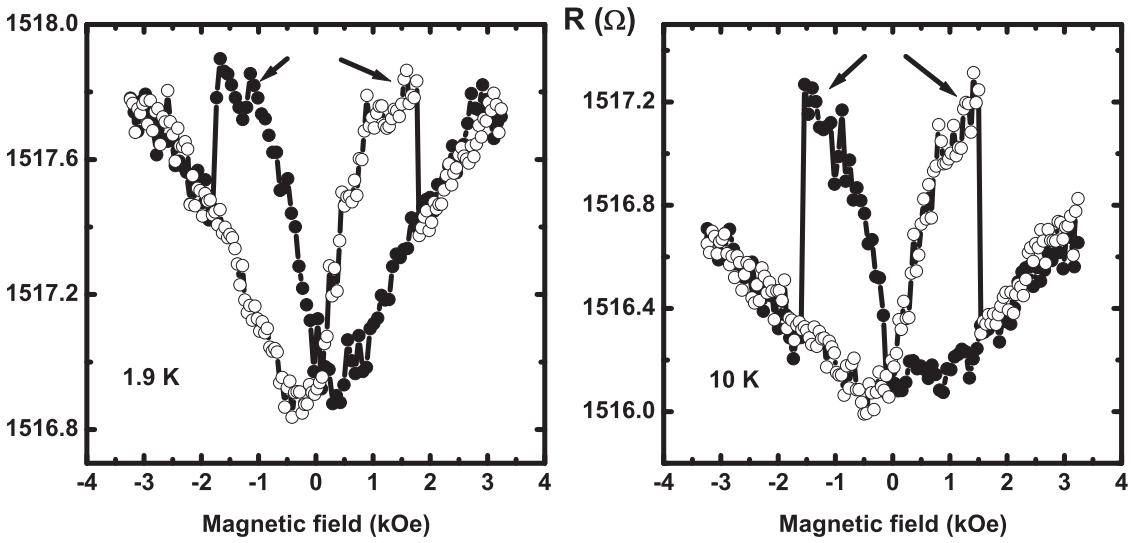

(a)

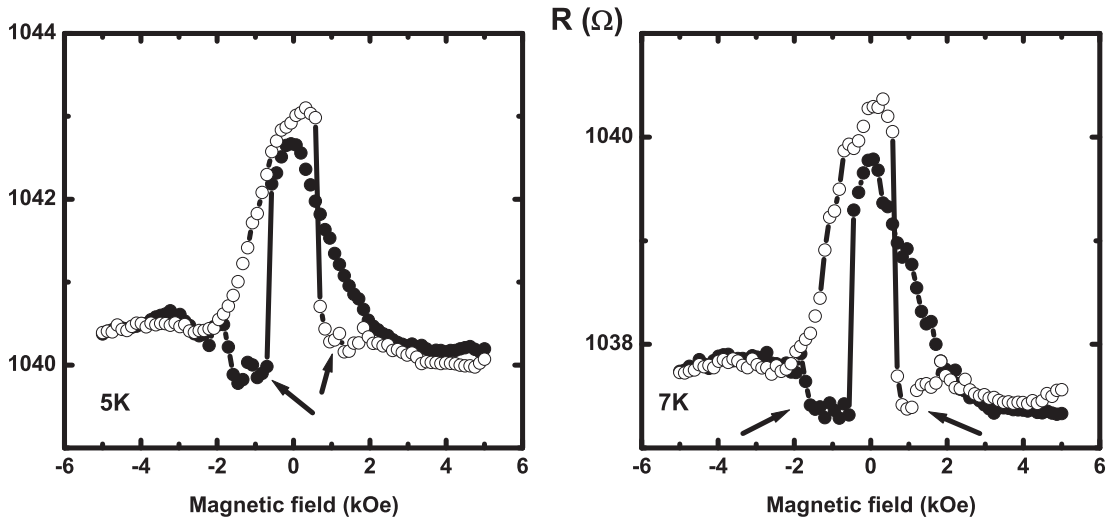

(b)

FIG. 2. Low-field-magnetoresistance characteristics of Ni-Alq_3-Co nanowire samples. (a) Typical normal spin-valve effect. The spin-valve peaks are indicated by arrows. These peaks are superimposed on a positive background magnetoresistance. The closed (open) circles indicate magnetic-field sweep from positive to negative (negative to positive) fields. The high-field characteristics of these samples are shown in Fig. 3. (b) Typical inverse spin-valve effect observed in Ni-Alq_3-Co nanowire spin valves, which are otherwise nominally identical to the samples showing the behavior as in (a). The spin-valve peaks are now inverted. There is a background negative magnetoresistance. Temperature and bias dependence of normal and inverse spin-valve signals are described in more detail in Refs. 15 and 16.

the samples showing *normal spin-valve* only. This difference in saturation fields can not be explained by the qualitative picture described below and indicates the necessity of quantitative modeling.

C. High-field magnetoresistance

In Fig. 3, we show the high-field-magnetoresistance data of the Ni-Alq_3-Co nanowire sample (exhibiting normal spin-valve effect) at two different temperatures. The background magnetoresistance shows an increasing trend even in the range where the magnetizations of the contacts are parallel (i.e., where the magnitude of the applied field is larger than 1800 Oe, which is the coercivity of the Co nanowire contact) and no further change is expected. Note that nickel nanowire contact has a lower coercivity of 800 Oe. As the magnitude of the magnetic field is increased, the "saturation knee" of the magnetoresistance curves occur at $\sim$20 kOe. This saturation field is relatively independent of temperature, at least in the range of 1.9–10 K. Although not visible on the scale of Fig. 3, each of these plots show a normal spin-valve effect in the low-field regime, i.e., between the coercive fields of Ni and Co nanowire electrodes [similar to those shown in Fig. 2(a)]. Presence of the spin-valve peaks confirms spin injection and transport in the organic layer.

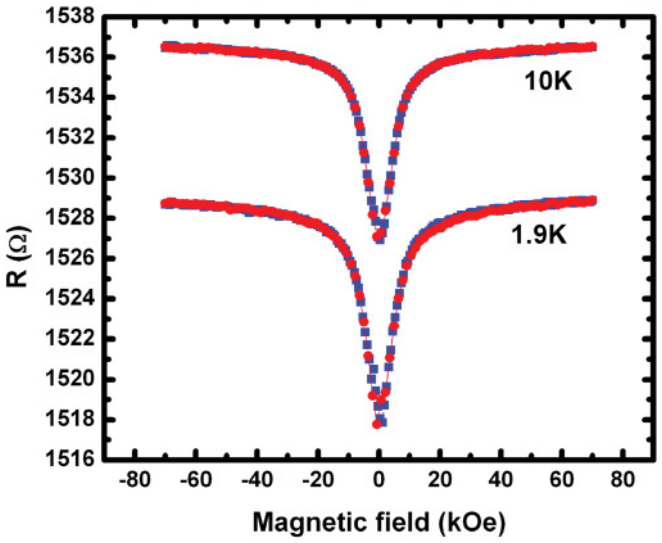

FIG. 3. (Color online) High-field-magnetoresistance characteristics of Ni-Alq_3-Co nanowire samples. The magnetic field is along the wire axis (i.e., parallel to the direction of current flow). The "saturation knee" occurs at ∼20 kOe and this value is relatively independent of temperature in our range of operation 1.9–10 K. The low-field magnetoresistance and spin-valve peaks of these samples are shown in Fig. 2(a). The 10-K plot has been shifted vertically upward by an amount of $\Delta = 9\Omega$ for clarity.

D. Control experiment I: Effect of ferromagnetic electrodes

First, we describe the high-field-magnetoresistance data of the control sample C_1, which does not contain any organic layer. Note that, unlike the trilayered spin-valve samples, preparation of this control sample requires *partial* removal of the barrier layer because of the fact that the resistivity of the ferromagnetic metals are nine orders of magnitude smaller than the organic layer and complete removal of the barrier layer will result in an essentially shorted device. This large difference in resistance at comparable bias indicates that the organic layer in the trilayered sample is nearly pinhole free. The current-voltage characteristics of these two classes are also qualitatively different. For the spin-valve samples, we obtain a nonlinear characteristic (similar to that reported in Ref. 15), whereas the control samples (C_1) show a linear ohmic behavior. Thus, the observed inversion of spin-valve peaks in our samples [Fig. 2(b)] can not be attributed to pinhole shorts.[50]

Using a previously reported procedure,[16] we have measured the magnetoresistance characteristics of approximately 500 bilayer ferromagnetic nanowires (Ni-Co) connected in parallel and capped by a thin cobalt layer. Figure 4(a) shows the high-field-magnetoresistance response of this sample when the field is parallel to the nanowire axis. The low-field data [inset of Fig. 4(a)] are featureless in the sense that there are no spin-valve-type peaks between the coercive fields of Ni and Co nanowires (i.e., between 800 and 1800 Oe). A similar response of template-grown ferromagnetic nanowires has been reported by other groups, e.g., Ref. 51. Lack of sharp switching in the anisotropic magnetoresistance (AMR) response can be attributed to the material and structural inhomogeneity of

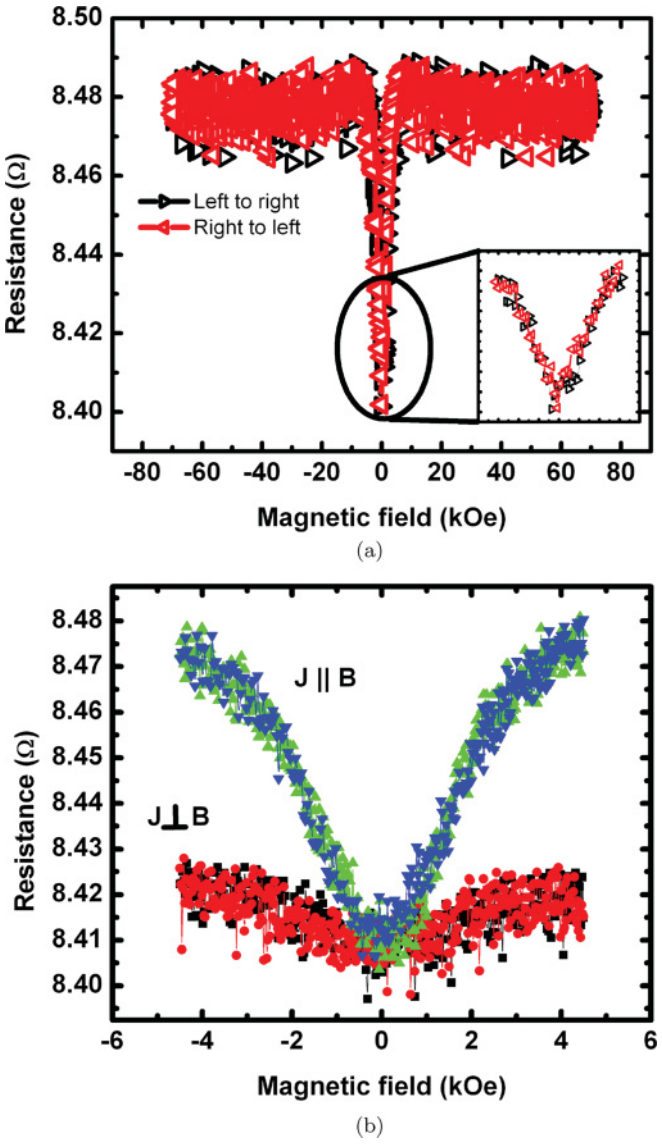

FIG. 4. (Color online) (a) High-field-magnetoresistance traces for the control samples (C_1, Ni-Co bilayer nanowires), which have no organic layer. The inset shows the magnified image at low field. As expected for these control samples, there is no spin-valve signal in the low-field region. The magnetoresistance saturates at ∼10 kOe. (b) Angular dependence of magnetoresistance. As expected, resistance in the parallel configuration is larger than the antiparallel configuration (Ref. 52). Note that the overall resistance is low ($\lesssim 10\ \Omega$) and the typical current-voltage characteristics (not shown) are linear, as expected.

the sample. Figure 4(b) shows the AMR data of the same sample for two orientations: (a) field parallel to current and (b) field perpendicular to current. As expected in the case of ferromagnets, the resistance in the parallel configuration is larger than the antiparallel configuration.[52]

The anisotropic magnetoresistance is always positive (i.e., $dR/d|B| > 0$, where R is the device resistance and B is the applied magnetic field), whereas, as shown before, some spin-valve samples exhibit a background *negative* magnetoresistance [Fig. 2(b)]. This, combined with the fact

that the resistance of these serially connected contacts are nine orders of magnitude smaller than the resistance of the Alq_3 layer, establishes that the observed background magnetoresistance of Ni-Alq_3-Co nanowires can never originate from the anisotropic magnetoresistance of the ferromagnetic nanowires.

E. Control experiment II: Possible presence of the local Hall effect or magneto-Coulomb effect

Magnetoresistance effects can also originate due to the local Hall effect[53] or magneto-Coulomb effect.[54] The local Hall effect, unlike the present case, mainly occurs in a planar spin-valve geometry where the fringing magnetic-field lines are normal to the direction of current flow in the paramagnetic layer. Signals due to these effects often mimic the spin-valve signal and may result in a background magnetoresistance. However, these signals persist even when only one contact is ferromagnetic. Therefore, we used Ag/Alq_3/Ni as the second set of control samples (C_2), which has only one ferromagnetic electrode. As shown in Fig. 5, we did not observe any background magnetoresistance or spin-valve peaks in these samples. We note that these control devices showed nonlinear current-voltage characteristics (Fig. 5) that are very similar to the working spin-valve devices.[15] So, the nonobservation of any magnetoresistance can not be explained simply by suspecting "shorted" devices. The absence of background magnetoresistance and spin-valve peaks in these control samples indicates that the effects observed in Ni-Alq_3-Co samples are indeed due to spin injection and transport and not because of any other artifact such as local Hall effect or magneto-Coulomb effect.

F. Proposed transport model

As described in Sec. II B, the negative results in the control experiments therefore indicate the necessity of invoking spin injection and transport for explaining the observed magnetoresistance behavior. The increasing trend and subsequent saturation of the device resistance with magnetic field in the range where magnetizations of both contacts are parallel (Fig. 3) can be explained by invoking the qualitative theory that was initially proposed to explain the correlation between the sign of the background magnetoresistance signal and the spin-valve peaks (Fig. 2).[16] There are two main ingredients of this model: First, we propose that spin relaxation takes place via the Elliott-Yafet mode, in which spin-diffusion length has an inverse dependence on magnetic field. This inverse dependence originates due to the fact that, in the presence of spin-orbit coupling, magnetic field enhances spin mixing and, as a result, momentum scattering events are accompanied by higher degrees of spin depolarization. Second, if the carriers resonantly tunnel via impurity states, the effective spin polarization of the nearest ferromagnetic contact is flipped (transport in Alq_3 occurs via hopping between molecular sites). In this case, one would observe an inverse spin-valve effect. This model of sign inversion of spin-valve peaks was first proposed in Ref. 55 in the context of nanoscale oxide tunnel junctions. Later, we used this model to explain sign inversion in nanowire organic spin valves.[16]

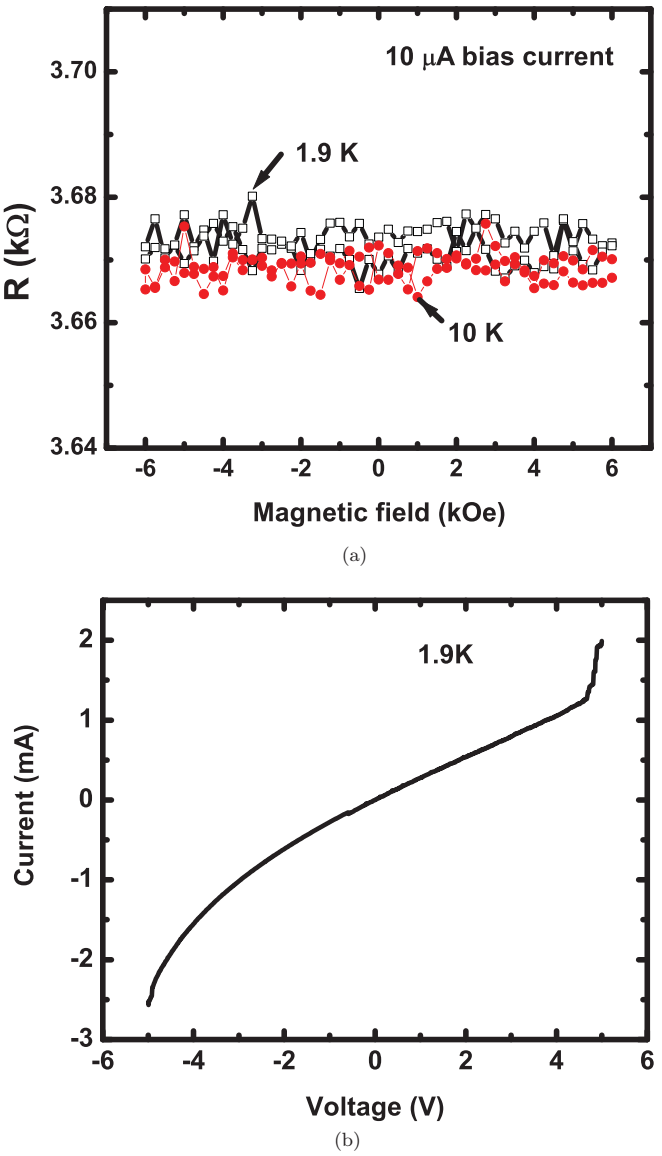

FIG. 5. (Color online) (a) Magnetoresistance measurements on Ag-Alq_3-Ni samples. No background magnetoresistance or spin-valve effect has been observed, which indicates that the observed effects in the previous pictures do not originate from any artifact due to local Hall effect or magneto-Coulomb effect. (b) Typical current-voltage characteristics of the Ag-Alq_3-Ni trilayered sample.

In our experiment, the Ni and Co contacts act as majority spin injector and detector. If, during transport, there is no resonant tunneling via impurity states (and no effective inversion of spin polarization of one of the contacts), the samples will show the normal spin-valve effect, i.e., $R_{AP} > R_P$ between the coercive fields of the contacts. At any other field, we observe that device resistance increases with $|B|$. This behavior can be explained as follows: As described in Sec. II A, the transmission probability of a spin-polarized carrier is proportional to $\cos^2\theta/2$, where θ is the mismatch angle between the detector magnetization and the spin moment arriving at the detector interface. Spin scattering events in the

organics randomize θ and tend to increase the device resistance compared to the $\theta = 0$ case (i.e., no spin relaxation). Now, if the Elliott-Yafet mechanism is dominant in the organic channel, increasing magnetic field will enhance the spin scattering rate (with a reduction in the spin-diffusion length) and further randomize θ. As a result, we expect to observe an increase in the device resistance with magnetic field (in the range where the magnetizations are parallel) and this is indeed what we see in Figs. 2(a) and 3. However, this increase should not continue indefinitely and must saturate at a field for which carriers are completely depolarized before arriving at the detector contact. Beyond this magnetic field, no further increase in device resistance will be observed and the resistance will saturate (say $R_{\max}$).

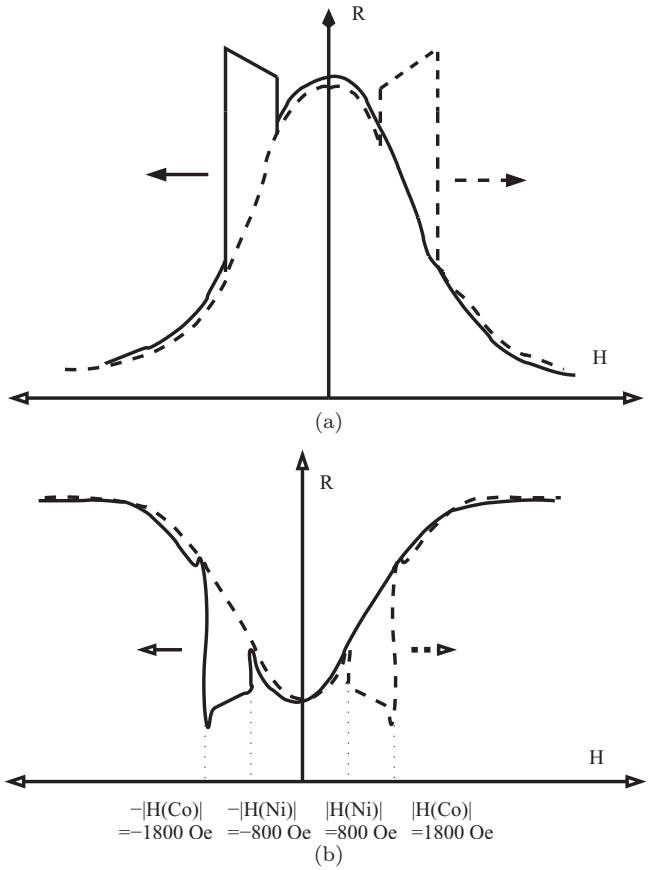

FIG. 6. Schematic description of the magnetoresistance traces for the *hypothetical* situation where hyperfine interaction is the dominant spin-relaxation mechanism. In such a case, spin-relaxation length increases with magnetic field. (a) Normal spin-valve effect. Here, the normal spin-valve effect (i.e., $R_{AP} > R_P$) is associated with *negative* background magnetoresistance and the resistance saturates to a minimum value at the high-field limit. (b) *Inverse* spin-valve effect, i.e., $R_{AP} < R_P$. Inverse behavior occurs due to effective inversion of spin polarization of one of the ferromagnets (as discussed in text). Here, the inverse spin-valve effect is associated with a positive background magnetoresistance and the resistance saturates to a maximum value in the high-magnetic-field limit. Clearly, both (a) and (b) contradict the observed behavior, i.e., Figs. 2 and 3, and therefore indicates that hyperfine interaction is not operative.

Note that Figs. 2 and 3 can not be explained by using hyperfine interaction as the dominant spin-relaxation mode. If hyperfine interaction is dominant, increasing magnetic field will reduce the spin scattering rate (since spins are now effectively pinned along $\pm\vec{B}$, with almost zero transition probability). In this case, increasing magnetic field should bring θ closer to zero, implying decreasing resistance. In such a case, the spin-valve response, as shown in Fig. 6(a), is expected. However, such a response has never been observed for any nanowire sample.

As mentioned before, for the samples showing inverse spin-valve effect, sign inversion occurs when injected carriers resonantly tunnel through some impurity state during transport. In this case, the ferromagnetic contact closest to the impurity exhibits an effective negative spin polarization. In the absence of any spin relaxation in the channel, $\theta \sim 180^\circ$ and the device resistance is high. Any spin relaxation in the channel will make $\theta < 180^\circ$, implying a smaller device resistance. If the Elliott-Yafet mechanism is operative, then increasing magnetic field will tend to randomize θ further, implying lower device resistance. This should show a negative magnetoresistance in the region where the bulk magnetizations of the ferromagnetic contacts are parallel. This is what we observe in Fig. 2(b). For these samples, there should exist a high-magnetic-field value for which device resistance saturates at a minimum value (say, $R_{\min}$). If hyperfine interaction is dominant, then increasing magnetic field should have exhibited higher device resistance at higher fields, i.e., positive background magnetoresistance, as schematically described in Fig. 6(b). This is also not exhibited by any nanowire devices.

We note that the ineffectiveness of the hyperfine interaction in the present case can also be understood from a simple order-of-magnitude estimate. A typical value of the hyperfine magnetic field is $\sim$5 mT, whereas in our samples we observe the spin-valve effect typically around $\sim$100 mT, which may be sufficient to pin the carrier spin orientations. However, this is the typical field strength in most Alq_3-based spin-valve devices reported in literature and, therefore, it is unlikely that hyperfine interaction is the dominant mechanism in any of these devices.

V. SUMMARY AND CONCLUSION

In conclusion, we have performed high-field-magnetoresistance measurements on Ni-Alq_3-Co nanowire devices. The magnetoresistance data in the high-field range (when both ferromagnetic contacts are magnetized parallel) can be used to shed light on the underlying spin-relaxation mechanism. These data support the transport model in which the Elliot-Yafet mode is the dominant spin-relaxation mechanism.

ACKNOWLEDGEMENT

This work was supported by the Disruptive Technology Challenge program (TRLabs, Canada) and the Discovery Grant program (NSERC, Canada).

*pramanik@ece.ualberta.ca

[1] M. Wohlgenannt, Synth. Met. **160**, 203 (2010).

[2] K. M. Alam and S. Pramanik, Chapter 4 in Nano-Semiconductors: Devices and Technology, edited by K. Iniewski, Taylor and Francis, 2011 (to appear).

[3] V. A. Dediu, L. E. Hueso, I. Bergenti, and C. Taliani, Nat. Mater. **8**, 707 (2009).

[4] *Organic Spintronics*, edited by Z. V. Vardeny (Taylor and Francis, London, 2010).

[5] S. Sanvito, Nat. Mater. **6**, 803 (2007).

[6] P. Ruden, Nat. Mater. **10**, 8 (2011).

[7] A. J. Drew, J. Hoppler, L. Schulz, F. L. Pratt, P. Desai, P. Shakya, T. Kreouzis, W. P. Gillin, A. Suter, N. A. Morley, V. K. Malik, A. Dubroka, K. W. Kim, H. Bouyanfif, F. Bourqui, C. Bernhard, R. Scheuermann, G. J. Nieuwenhuys, T. Prokscha, and E. Morenzoni, Nat. Mater. **8**, 109 (2009).

[8] L. Schulz, L. Nuccio, M. Willis, P. Desai, P. Shakya, T. Kreouzis, V. K. Malik, C. Bernhard, F. L. Pratt, N. A. Morley, A. Suter, G. J. Nieuwenhuys, T. Prokscha, E. Morenzoni, W. P. Gillin, and A. J. Drew, Nat. Mater. **10**, 39 (2011).

[9] M. Cinchetti, K. Heimer, J. Wüstenberg, O. Andreyev, M. Bauer, S. Lach, C. Ziegler, Y. Gao, and M. Aeschlimann, Nat. Mater. **8**, 115 (2009).

[10] N. Atodiresei, J. Brede, P. Lazic, V. Caciuc, G. Hoffmann, R. Wiesendanger, and S. Blügel, Phys. Rev. Lett. **105**, 066601 (2010).

[11] J. Brede, N. Atodiresei, S. Kuck, P. Lazic, V. Caciuc, Y. Morikawa, G. Hoffmann, S. Blügel, and R. Wiesendanger, Phys. Rev. Lett. **105**, 047204 (2010).

[12] V. Dediu, M. Murgia, F. C. Matacotta, C. Taliani, and S. Barbanera, Solid State Commun. **122**, 181 (2002).

[13] Z. H. Xiong, D. Wu, Z. Valy Vardeny, and J. Shi, Nature (London) **427**, 821 (2004).

[14] T. S. Santos, J. S. Lee, P. Migdal, I. C. Lekshmi, B. Satpati, and J. S. Moodera, Phys. Rev. Lett. **98**, 016601 (2007).

[15] S. Pramanik, C-G. Stefanita, S. Patibandla, S. Bandyopadhyay, K. Garre, N. Harth, and M. Cahay, Nat. Nanotechnol. **2**, 216 (2007).

[16] S. Pramanik, S. Bandyopadhyay, K. Garre, and M. Cahay, Phys. Rev. B **74**, 235329 (2006).

[17] V. Dediu, L. E. Hueso, I. Bergenti, A. Riminucci, F. Borgatti, P. Graziosi, C. Newby, F. Casoli, M. P. De Jong, C. Taliani, and Y. Zhan, Phys. Rev. B **78**, 115203 (2008).

[18] Y. Liu, S. M. Watson, T. Lee, J. M. Gorham, H. E. Katz, J. A. Borchers, H. D. Fairbrother, and D. H. Reich, Phys. Rev. B **79**, 075312 (2009).

[19] F. J. Wang, C. G. Yang, Z. V. Vardeny, and X. G. Li, Phys. Rev. B **75**, 245324 (2007).

[20] S. Majumdar, H. S. Majumdar, R. Laiho, and R. Österbacka, J. Alloys Compd. **423**, 169 (2006).

[21] W. Xu, G. J. Szulczewski, P. LeClair, I. Navarrete, R. Schad, G. Miao, H. Guo, and A. Gupta, Appl. Phys. Lett. **90**, 072506 (2007).

[22] C. Barraud, P. Seneor, R. Mattana, S. Fusil, K. Bouzehouane, C. Deranlot, P. Graziosi, L. Hueso, I. Bergenti, V. Dediu, F. Petroff, and A. Fert, Nat. Phys. **6**, 615 (2010).

[23] T. D. Nguyen, G. Hukic-Markosian, F. Wang, L. Wojcik, X-G. Li, E. Ehrenfreund, and Z. V. Vardeny, Nat. Mater. **9**, 345 (2010).

[24] R. Lin, F. Wang, J. Rybicki, M. Wohlgenannt, and K. A. Hutchinson, Phys. Rev. B **81**, 195214 (2010).

[25] J-W. Yoo, H. W. Jang, V. N. Prigodin, C. Kao, C. B. Eom, and A. J. Epstein, Phys. Rev. B **80**, 205207 (2009).

[26] J-W. Yoo, C-Y. Chen, H. W. Jang, C. W. Bark, V. N. Prigodin, C. B. Eom, and A. J. Epstein, Nat. Mater. **9**, 638 (2010).

[27] S. Patibandla, B. Kanchibotla, S. Pramanik, S. Bandyopadhyay, and M. Cahay, Int. J. Nanotechnol. Mol. Comput. **1**, 20 (2009).

[28] R. J. Elliott, Phys. Rev. **96**, 266 (1954).

[29] A. Abragam, *The Principles of Nuclear Magnetism* (Clarendon, Oxford, 1961).

[30] A. V. Khaetskii, D. Loss, and L. Glazman, Phys. Rev. Lett. **88**, 186802 (2002).

[31] M. I. D'yakonov and V. I. Perel', Zh. Eksp. Teor. Fiz. **60**, 1954 (1971) [Sov. Phys. JETP **33**, 1053 (1971)]; M. I. D'yakonov and V. I. Perel', Fiz. Tverd. Tela. **13**, 3581 (1971) [Sov. Phys. Solid State **13**, 3023 (1972)].

[32] *Optical Orientation*, edited by F. Meier and B. Zakharchenya (North Holland Physics Publishing, Elsevier, 1984), Chap. 3.

[33] B. I. Shklovskii, Phys. Rev. B **73**, 193201 (2006).

[34] K. Tarafder, B. Sanyal, and P. M. Oppeneer, Phys. Rev. B **82**, 060413 (R) (2010).

[35] Z. G. Yu, Phys. Rev. Lett. **106**, 106602 (2011).

[36] P. A. Bobbert, W. Wagemans, F. W. A. van Oost, B. Koopmans, and M. Wohlgenannt, Phys. Rev. Lett. **102**, 156604 (2009).

[37] N. J. Rolfe, M. Heeney, P. B. Wyatt, A. J. Drew, T. Kreouzis, and W. P. Gillin, Phys. Rev. B **80**, 241201 (2009).

[38] F. Kuemmeth, S. Ilani, D. C. Ralph, and P. L. McEuen, Nature (London) **452**, 448 (2008).

[39] I. Zutic, J. Fabian, and S. DasSarma, Rev. Mod. Phys. **76**, 323 (2004).

[40] S. Bandyopadhyay, Phys. Rev. B **81**, 153202 (2010).

[41] D. Wu, Z. H. Xiong, X. G. Li, Z. V. Vardeny, and J. Shi, Phys. Rev. Lett. **95**, 016802 (2005).

[42] E. Y. Tsymbal, O. N. Mryasov, and P. R. LeClair, J. Phys. Condens. Matter **15**, R109 (2003).

[43] S. Bandyopadhyay and M. Cahay, Nanotechnology **20**, 412001 (2009).

[44] Ö. Mermer, G. Veeraraghavan, T. L. Francis, Y. Sheng, D. T. Nguyen, M. Wohlgenannt, A. Köhler, M. K. Al-Suti, and M. S. Khan, Phys. Rev. B **72**, 205202 (2005).

[45] Ö. Mermer, G. Veeraraghavan, T. L. Francis, and M. Wohlgenannt, Solid State Commun. **134**, 631 (2005).

[46] S. Pramanik *et al.* (unpublished).

[47] A. P. Bonifas and R. L. McCreery, Nat. Nanotechnol. **5**, 612 (2010).

[48] J. C. Walker, R. Droste, G. Stern, and J. Tyson, J. Appl. Phys. **55**, 2500 (1984).

[49] F. J. Wang, Z. H. Xiong, D. Wu, J. Shi, and Z. V. Vardeny, Synth. Met. **155**, 172 (2005).

[50] S. Mukhopadhyay and I. Das, Phys. Rev. Lett. **96**, 026601 (2006).

[51] T. Ohgai, L. Gravier, X. Hoffer, M. Lindeberg, K. Hjort, R. Spohr, and J.-Ph. Ansermet, J. Phys. D: Appl. Phys. **36**, 3109 (2003).

[52] T. R. McGuire and R. I. Potter, IEEE Trans. Magn. **MAG-11**, 1018 (1975).

[53] F. G. Monzon and M. L. Roukes, J. Magn. Magn. Mater. **198-199**, 632 (1999).

[54] S. J. van der Molen, N. Tombros, and B. J. van Wees, Phys. Rev. B **73**, 220406(R) (2006).

[55] E. Y. Tsymbal, A. Sokolov, I. F. Sabirianov, and B. Doudin, Phys. Rev. Lett. **90**, 186602 (2003).